International Journal of Fluid Machinery and Systems
Vol. 8, No. 4, October-December 2015

DOI: 10.5293/IJFMS.2015.8.4.254
ISSN (Online): 1882-9554

Original Paper

The effect of materials properties on the reliability of hydraulic turbine runners

Denis Thibault[1], Martin Gagnon[1] and Stéphane Godin[1]

Institut de recherche d'Hydro-Québec (IREQ),
Varennes, Québec, J4J 5J9, thibault.denis@ireq.ca
gagnon.martin@ireq.ca, godin.stephane@ireq.ca

Abstract

The failure of hydraulic turbine runners is a rare event. So in order to assess the reliability of these components one cannot rely solely on the number of observed failures in a given population. However, as there is a limited number of degradation mechanisms involved, it is possible to use physically-based reliability models. Such models are often more complicated but are able to account for physical parameters in the degradation process. They can therefore help provide solutions to improve reliability. With such models, the effect of materials properties on runner reliability can be highlighted. This paper presents a brief review of the Kitagawa-Takahashi diagram which links the damage tolerance approach, based on fracture mechanics, to the stress or strain-life approaches. Using simplified response spectra based on runner stress measurements, we will show how fatigue reliability is sensitive to materials fatigue properties, namely fatigue crack propagation behaviour and fatigue limit obtained on S-N curves. Furthermore, we will review the influence of the main microstructural features observed in 13%Cr-4%Ni stainless steels commonly used for runner manufacturing. The goal is ultimately to identify the most influential microstructural features and to quantify their effect on fatigue reliability of runners.

Keywords: fatigue, reliability, stainless steel, hydraulic turbine, turbine runner, microstructure

1. Introduction

Turbine runners fatigue properties have received a lot of attention in the recent years. This renewed interest is due to a combination of factors. First, power plants owners want turbines with a longer lifespan. Since blade fatigue cracking is one of the predominant degradation mechanisms, designers need to ensure that the runner will endure its expected lifespan without cracking. Secondly, numerical tools improvement and continuous demand for better turbine performances tend to push new runner designs closer to the materials limits. This, in turn, demands a better understanding of materials behaviour. Thirdly, the importance of cracking events is exacerbated by the pressure put on the plant operator to increase the availability of turbine-generator units. In the past, repairs could be done recurrently during scheduled downtime, but as this downtime is now more and more limited, there is less opportunity to repair cracks without production lost. Finally, we should include the change in turbine operation (e.g. increasing number of starts-stops and power output variations) combined with the need to maximize the lifespan of the important fleet of turbines installed in the 70's and in the 80's that are now approaching their expected life expectancies.

To assess turbine runners fatigue reliability, the starting point is a proper failure criterion. Because long cracks can develop in runners without incurring safety issues, the main concerns for turbine operators are repair cost and downtime. This leads us to a failure criterion defined as the point where high frequency/low amplitude stress cycles start to contribute to crack propagation [1]. Those high frequency/low amplitude loads are referred to as high cycle fatigue loads (HCF) as opposed to low cycle fatigue loads (LCF) which represents the low frequency/high amplitude loads. We consider that an initial defect exists and that the LCF loads are contributing to its propagation. We state that as soon as the HCF loads contribute to crack propagation, the crack will rapidly become detectable and it will have to be repaired. Given this failure criterion, we use the Kitagawa-Takahashi diagram [2] to quantify the probability of a given defect to cross the limit-state i.e. to propagate rapidly. This model was presented in details in previous publications [1, 3-5] and is briefly introduced in the following sections.

Received January 15 2015; revised July 30 2015; accepted for publication Octoberber 15 2015: Review conducted by Prof. Yoshinobu Tsujimoto. (Paper number O15054S)
Corresponding author: Denis Thibault, thibault.denis@ireq.ca

This paper was presented at the 27th IAHR Symposium on Hydraulic Machinery and Systems, September 4, Montreal, Canada.

To assess fatigue reliability using this physically-based model, three inputs are needed:

- the highest expected HCF load in a given volume and its uncertainty;
- the largest expected flaw size in a given volume and its uncertainty;
- the limit-state parameters and their uncertainties.

The limit state is in fact defined by two parameters: the fatigue limit from the S-N curves ($\Delta\sigma_0$) and the fatigue crack growth threshold as defined by linear elastic fracture mechanics (referred to as ΔKth).

These last inputs i.e. $\Delta\sigma_0$ and ΔKth are influenced by loading (stress ratio, overload, loading mode), environment, temperature, residual stress and by material properties. The first three parameters can seldom be controlled during manufacturing, while the last two (residual stress and material properties) can be improved by choosing an optimized alloy for runner fabrication. Note that repair processes and procedures also have an influence on these parameters. This raises two questions:

- Can we significantly improve fatigue reliability?
- Can we improve it through the material properties?

To tackle the first question, a sensitivity study is presented using the reliability model previously introduced. In this sensitivity study, a simplified load spectrum will be used as an input and the limit state parameters will be modified to observe their effects on the runner fatigue reliability. The second question will be addressed from a metallurgical standpoint by reviewing the different microstructural features of the typical alloy used for runner fabrication. The studied alloy is 13%Cr-4%Ni soft martensitic stainless steel. This encompasses the cast alloy CA6NM, its wrought and forged counterpart AISI 415 and F6NM and the welding filler material AWS 410NiMo . Finally, insights on how these different features can affect fatigue properties are discussed.

2. The relation between materials properties and fatigue reliability

2.1 The Kitagawa-Takahashi diagram and how it is related to materials properties

The Kitagawa-Takahashi diagram was first introduced in 1976 [2] to illustrate how the ΔK_{th} in high strength steel tends to decrease when crack length decreases. Plotting their results of short fatigue crack growth testing on a stress range ($\Delta\sigma$) versus crack length (a) the authors found that the stress range threshold decreased when crack length was lower than 0.13mm and then reached a plateau (see Figure 1). This plateau corresponds to the fatigue limit ($\Delta\sigma_0$) determined by S-N curves.

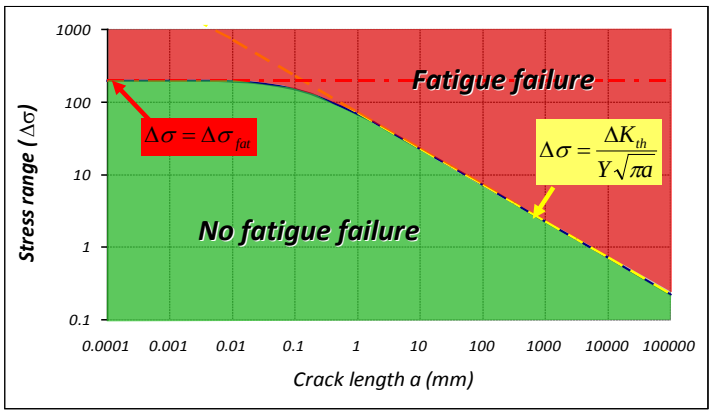

Figure 1. Kitagawa-Takahashi diagram example

This diagram illustrates how classical approaches based on S-N curves can be linked to damage tolerance approaches based on fracture mechanics. It also shows which material properties need to be studied to assess fatigue behaviour of structures. These properties are: the fatigue resistance ($\Delta\sigma_0$) and the crack growth threshold (ΔK_{th}). The diagram can also be extended to include other parameters such as notch effect [6], multi-axial criteria [7] and residual stresses [8, 9]. In the following section we use the probabilistic extension presented in previous publications illustrated in Figure 2 [1, 3-5].

It is relevant to note that the joint distribution formed by the defect size and stress range as illustrated on Figure 2 evolves toward the right-hand side of the graph as low-cycle fatigue loads contribute to crack growth. The consequence of crack propagation under LCF loads is an increase of defects size over time. This is due to the LCF stress range which is above the crack growth threshold and located in the Paris regime of the crack propagation curve i.e. in the stable crack growth regime. Hence, as the runner operates, its fatigue reliability will decrease as the joint probability distribution depicted in Figure 2 approaches the failure boundary. One conclusion that has to be underlined is that the reliability decreasing rate is mostly related to the LCF loads. The value of $\Delta\sigma_0$ also decreases with the number of HCF cycles which might also influence fatigue reliability decreasing rate in some instances. However, $\Delta\sigma_0$ will tend to stabilise after 1e7 cycles.

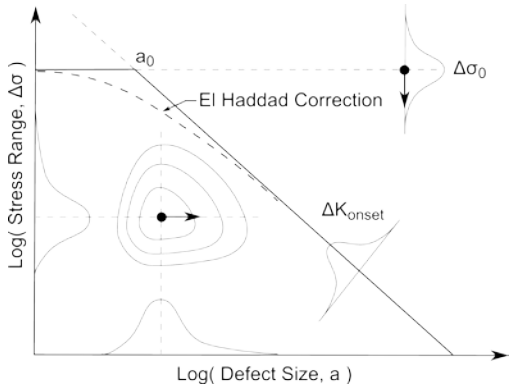

Figure 2. Probabilistic Kitagawa-Takahashi diagram

2.2 Sensitivity study

To illustrate the effect of $\Delta\sigma_0$ and ΔK_{th} on runner fatigue reliability, a simplified load spectrum representative of allowable stresses on a low head Francis turbine was used. This simplified spectrum consists of superimposed high frequency HCF loads on a low frequency LCF load (see Figure 3). The inputs parameters used for this sensitivity study are detailed in Table 1.

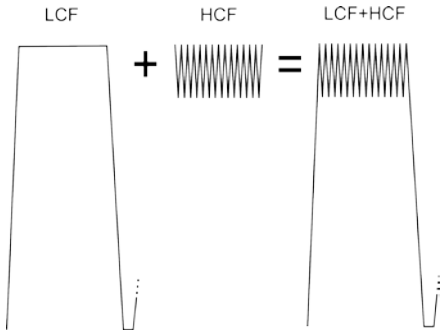

Figure 3. Simplified load spectrum

Table 1. Sensitivity study initial parameters

	Location	Scale	Distribution	Units
ΔK_{th}	2.0[a]	-	-	MPa $m^{1/2}$
$\Delta\sigma_0$	50	-	-	MPa
a	1.5[b]	0.5	Gumbel	mm
σ_{LCF}	200.0	-	-	MPa
σ_{HCF}	20.0	1.0	Gumbel	MPa
N_{LCF}	1	-	-	day-1

[a]Crack propagation data are taken from the British standard BS7910 [10]
[b]The defect is taken as a corner flaw

To quantify the effect of material properties on reliability, we first looked at the influence of ΔK_{th}. We used an initial value of $2\,MPa\sqrt{m}$, representing the proposed value in the British Standard BS7910 [10]. This lower bound value was then increased to $3\,MPa\sqrt{m}$ and then to $4\,MPa\sqrt{m}$, those two values representing possible threshold values for 13%Cr-4%Ni steels [3, 11-14]. The resulting effect on reliability can be seen in Figure 4a. In this graph, the reliability index is the Hasofer-Lind reliability index (β) as described in [1]. The probability of failure (P_f) represents the probability of one blade having a crack. The overall probability (R) of a runner having no cracked blades can be approximated by:

$$R = (1 - P_f)^n$$
$$P_f = \Phi(-\beta)$$

Where n is the number of blades of the runner and Φ is the standard cumulative function. We thus observe on Figure 4a that a variation in ΔK_{th} has an enormous importance on the initial reliability index i.e. the index determined at turbine commissioning (or whenever the first assessment is made). This index decreases with time, or more precisely with each LCF load. In this case, given enough time, the indexes for the different ΔK_{th} tend to merge. This however is only true after the expected lifespan of the turbine

is spent (50 to 70 years). To quantify the effect of different ΔK_{th} on reliability over time, the probability of failure at 60 years can be computed and compared. We find that the probability of finding a crack on one blade (P_f) after 60 years is respectively around 1/10, 1/200 and 1/3000 when the ΔK_{th} is increased from 2 $MPa\sqrt{m}$ to 3 $MPa\sqrt{m}$ and to 4 $MPa\sqrt{m}$.

The same exercise was made for the fatigue endurance limit $\Delta\sigma_0$. The limit was changed from the initial value of 50MPa up to 400MPa to illustrate its effect on the reliability over time. These values represent a possible range of fatigue limits depending on the conditions and the security factor used for calculations [3]. The results are presented in Figure 4b. It can be seen that the curves are almost superimposed for the highest values of $\Delta\sigma_0$ namely 400MPa, 200MPa and 100MPa. Differences are however seen for 100MPa and the lowest value of 50MPa. If we compare the probability of failure after 60 years in operation we find P_f values between 1/30 and 1/60 for the three highest values of $\Delta\sigma_0$ and around 1/10 for $\Delta\sigma_0$ = 50MPa.

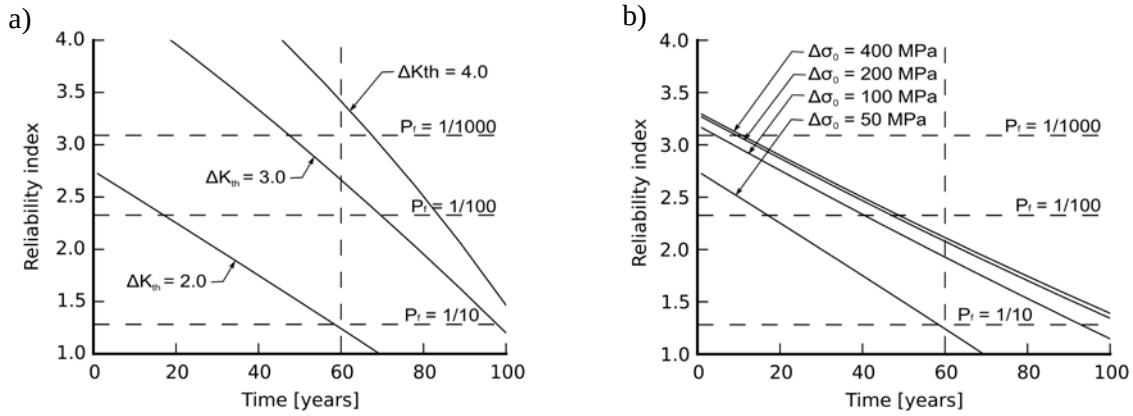

Figure 4. Reliability index variation over time
a) for different values of ΔK_{th} b) for different fatigue resistance limits ($\Delta\sigma_0$)

Another property that can be modified is the fatigue crack growth rate in the Paris region i.e. in the stable crack growth regime of the crack growth curve. Changing this growth rate will not change the initial reliability index but will change the effect of the LCF loads, that is to say the rate at which this index decreases over time. Taking two values corresponding to actual crack propagation rates measured in labs for as-welded and post-weld heat treated (PWHT) 410NiMo, we can compare their effect on reliability to the initial curve calculated using the propagation curve found in the British Standards [10]. The propagation curves used for this comparison are presented in Figure a. The results of the reliability comparison are presented in Figure b. It can be seen that the observed differences in crack growth behaviour before and after post-weld heat treatment have an important effect on long time runners reliability. If we again compare the probability of finding a crack in one blade after 60 years of operation, we find a P_f value around 1/100 for the tempered alloy, around 1/20 for the as-welded alloy and 1/10 if the curve from the BS7910 standard is used. As can be seen in Figure b, these disparities will tend to increase over time.

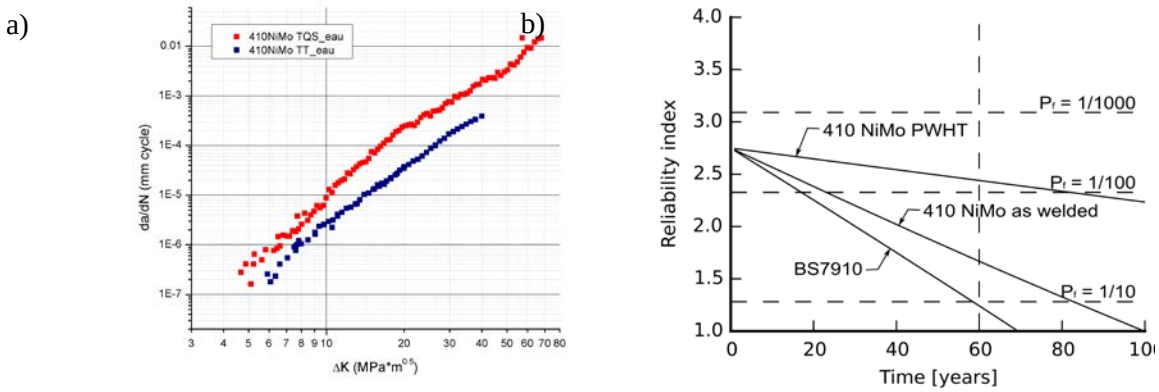

Figure 5. Reliability index evolution over time for different values of crack growth rate

The results of this sensitivity study underline the importance of understanding the real conditions in which turbine runners operate to correctly set $\Delta\sigma_0$ and ΔK_{th}. Choosing adequate values for the limit state is a challenging task that can be addressed by using an interval to reflect the inherent uncertainty related to materials properties. As introduced in a previous paper [3], three domains have been defined on the Kitagawa-Takahashi diagram using the lowest and highest possible values of $\Delta\sigma_0$ and ΔK_{th} as shown in Figure 6. The first domain is considered the "Safe" region and represents the area inside which we believe that crack growth is not possible. There is also the "unsafe" area where we are certain that crack growth will occur. Finally there is the uncertainty interval inside which the limit state should be located. Since the uncertainty interval is delimited by the lowest and highest value believed possible, the area is larger than what should be considered probable given better knowledge of both the material microstructural features and their influences on our limit state. The next section will give a brief overview of the most important microstructural features of 13%Cr-4%Ni and their effect on fatigue in an effort to define probable values of our limit state.

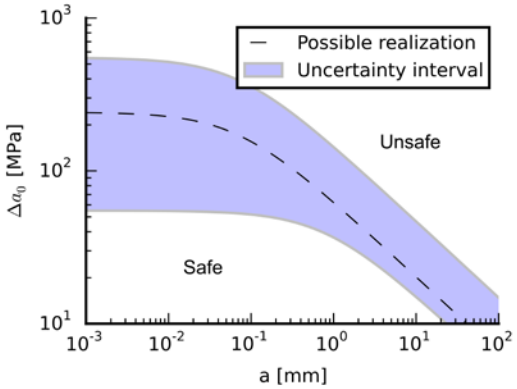

Figure 6. Limit state uncertainty interval illustrated on a Kitagawa-Takahashi diagram

3. The microstructural features of 13%Cr-4%Ni martensitic stainless steel and their potential effect on fatigue

3.1 Generalities

CA6NM has been used extensively for turbine runner manufacturing since its development in the sixties [15]. This low-carbon soft martensitic stainless steel has a high strength, good corrosion and cavitation resistance, and a high toughness. This cast alloy has replaced CA15 in many applications because it is easier to process in the foundry and because it has a better weldability [16]. This improved weldability is mainly due to the lower carbon content (0.06% instead of 0.15%). The lower carbon content is compensated by a higher nickel content to keep the Cr_{eq}/Ni_{eq} constant. The phase transformations occurring in this alloy when it solidifies and cools down can be illustrated by a pseudo-binary phase diagram (Cr-Ni)-Fe in which a Cr/Ni ratio of 3 is kept constant. The AISI 415 is essentially the same alloy as CA6NM but is produced by hot-rolling in the austenite stage. Most of the time, CA6NM and AISI 415 are welded using AWS 410NiMo which is a filler material having similar chemical composition and similar microstructural features.

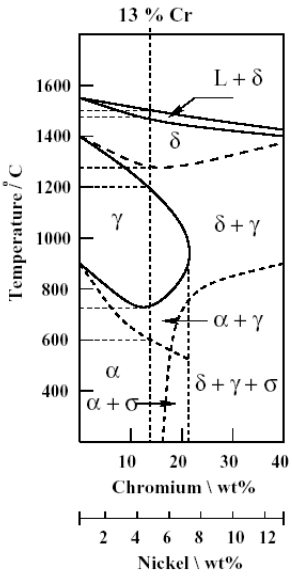

Figure 5. Pseudo-binary (Cr-Ni)-Fe phase diagram (Cr/Ni = 3). The dashed line at 13%Cr corresponds to the CA6NM, AISI415 and 410NiMo composition (from Folkhard [17])

At room temperature, the as-quenched alloy consists essentially of laths martensite but can also contain a small amount of δ-ferrite [18]. The cooling rate does not play an important role as it normally does with martensitic steel: only one phase forms for cooling time ranging from 20 seconds to 24 hours [19], so thick sections can be air-cooled and still be fully martensitic. CA6NM is normally used in the tempered state. During tempering between 565°C and 620°C, some of the martensite transforms back to austenite. This austenite gets enriched in nickel and is thus stable when the alloy is cooled back to room temperature. Depending on tempering time, temperature and the exact chemical composition of the alloy, as much as 25% reformed austenite can be found after tempering [18, 20, 21].

3.2 Grain size (prior austenite, martensite packets, etc)

As with any metallic alloy, one of the most important microstructural parameter that has to be investigated is the grain size. If the definition of a crystallographic grain is quite clear for austenitic or ferritic microstructure, it is more complex when it comes to martensitic structures. The grain can refer to many different microstructural features that are revealed with chemical or electrochemical etching (see Figure 6). The first one being the prior austenite grain (referred as parent austenite grain) which is the grain forming from ferrite at high temperature (starting around 1300°C). From this parent grain, martensite laths nucleate and grow heterogeneously with particular orientations. The martensite laths can be regrouped by blocks that represent a group of laths having the same orientation and packets which are a group of laths having almost the same habit plane. So, a prior austenite grain can be divided in different packets that are themselves divided in different blocks of laths. [22, 23]

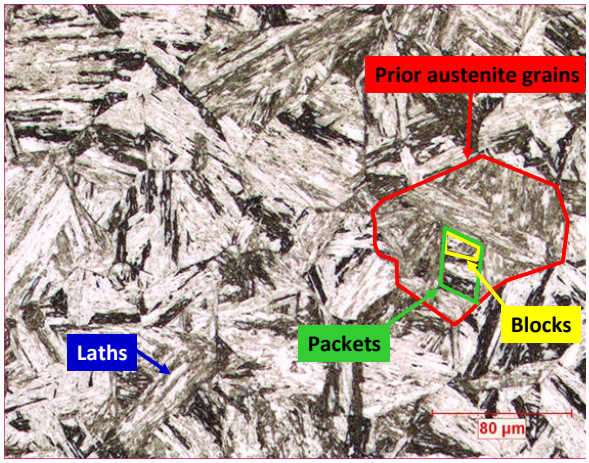

Figure 6. A typical tempered microstructure of 13%Cr-4%Ni stainless steel as seen by optical microscopy (500x)

These features are recognized as being directly related to the mechanical properties of martensitic structures [24-27]. But for fatigue crack growth properties, even if it is usually admitted that for austenitic, ferritic and pearlitic steels, larger grain sizes mean higher values of ΔK_{th} [28-32], this relation is not as clear for martensitic structures. Different studies have come to contradictory conclusions [33-36] on this subject. For the 13%Cr-4%Ni specifically, Trudel et al. found that differences in crack growth rate between a tempered weld and its base metal at low and mid-range ΔK could partly be explained by crack path tortuosity that was due to the coarser microstructure of the base metal [37]. In a previous study, we observed by fractographic analyses that cracks tend to grow at packet boundaries in cast and in wrought 13%Cr-4%Ni stainless steel near ΔK_{th} [38]. So it seems that for 13%Cr-4%Ni, the martensite packets boundaries play a significant role in crack propagation, a role that needs to be better understood and quantified.

3.3 Reformed austenite

As was noted in the previous section, the as-quenched martensite in 13%Cr-4%Ni alloys transforms back to austenite during tempering. This reformed austenite grows by a diffusional process [39]. It is finely dispersed in the martensitic matrix and cannot be resolved by optical microscopy; it can however be observed by scanning electron microscopy (Figure 7). It is normally recognized that this reformed austenite found in tempered 13%Cr-4%Ni stainless steel helps to increase their Charpy impact resistance [40, 41]. This austenite is richer in Ni than the surrounding matrix [41, 42]. A part of this austenite is mechanically unstable and can transform to martensite during tensile and during impact tests [18, 40, 43]. Recent studies pointed out that the hardness of the martensite matrix could also play an important role in the stability of this austenite and hence on the mechanical properties [42] of these alloys. It has also been showed that this reformed austenite transforms during fatigue crack propagation at near threshold values [14]. Recent results showed that this transformation could increase the ΔK_{th} in 13%Cr-4%Ni [44].

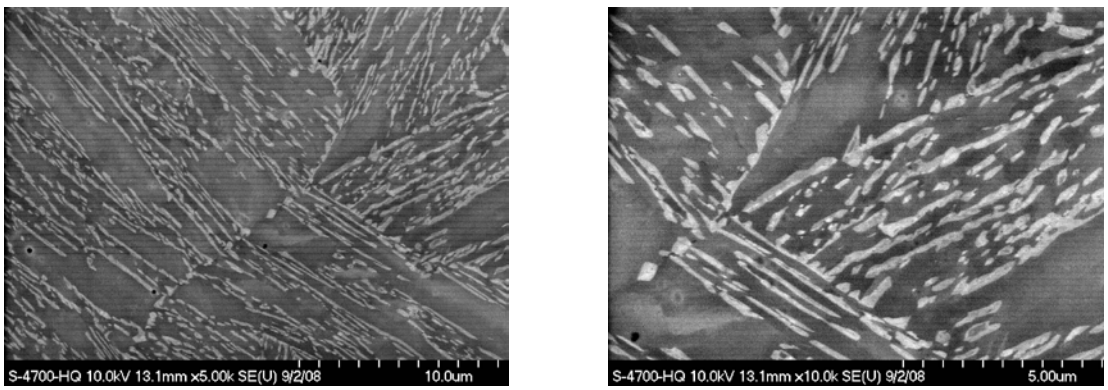

Figure 7. Reformed austenite lamellae as seen by scanning electron microscopy
a) 5000x b) 10 000x

3.4 δ ferrite

As pointed out previously, 13%Cr-4%Ni stainless steel oftentimes contain some ferrite at room temperature. The presence of this phase can be explained by inapropriate chemical compositions or, more frequently, by non-equilibrium solidification conditions. As solidification during welding is far from equilibrium conditions, welds made with 410NiMo often contain δ-ferrite. A recent study has shown that the presence of δ-ferrite can lower impact properties of 13%Cr-4%Ni CA6NM, mostly by increasing the ductile to brittle transition obtained by Charpy V-notch impact testing [45]. Carrouge et al. had previously come to the same conclusion when they tested a supermartensitic steel having a similar microstructure [46]. It seems that the effect of this phase on $\Delta\sigma_0$ or on ΔK_{th} have not yet been investigated in martensitic stainless steels.

3.5 Oxides and other inclusions

Some studies found that oxides and other inclusions have an adverse effect on fatigue crack propagation in different alloys [47]. While others found no effect on the threshold value but a detrimental effect on the fatigue limit [48]. This effect of inclusions on the fatigue limit is in fact generally accepted [49], [50]. Murakami et al. observed that the fatigue limit of bearing steel tended to increase as the size of inclusions decreased over the years due to better steelmaking practices [51]. For 13%Cr-4%Ni steels, silicon and aluminum complex oxides are found in different proportion and sizes. In 410NiMo welds, the inclusion type and size will depend on the welding process and procedures. The effects of these oxides on fatigue properties of 13%Cr-4%Ni stainless steel have yet to be investigated.

4. Most probable values vs the uncertainty interval from possible values

These microstructural features all contribute to the uncertainty of the previously defined limit state for fatigue reliability. The conservative approach consists in using values defined in standards and codes, for example the values of ΔK_{th} given in BS7910 [10] and values $\Delta\sigma_0$ proposed or corrected following ASME codes [52]. Those conservative values are used to define the "Safe" zone. With a better knowledge of both the structure response spectra and the alloy actually used during manufacturing, including its metallurgical state, it is possible to define a probable interval narrower than the uncertainty interval from possible values presented in Figure 6 .

For example, taking the loading parameters of the sensitivity study we can define probable minimum and maximum values of $2.2\,MPa\sqrt{m}$ and $3.9\ MPa\sqrt{m}$ for ΔK_{th} from the available data in the litterature. A fatigue resistance probable interval can also be defined taking fatigue resistance values at N = 1e9 as this would be more representative of the expected number of cycles for a low head Francis turbine. The values used for the most probable interval inside which we expect the limit state are shown in Table 2. Figure 8a illustrates the Kitagawa-Takahashi diagram with both the possible interval and the most probable interval.

Using these values, we can calculate the evolution of the reliability index over time. In Figure 10b, we observe that a small change in ΔK_{th} and $\Delta\sigma_0$ has a significant effect on the interval inside which we can expect the reliability index. In a similar manner, the uncertainty intervals could be further refined to represent confidence interval, risk level or belief to help decision maker during risk assessment [53].

Table 2. Values used to define the most probable uncertainty interval

	Min value	Max value	Description	Source
ΔK_{th}	$2.2\,MPa\sqrt{m}$	$3.9\,MPa\sqrt{m}$	For R > 0.5, values found by different authors	[13, 54, 55]
$\Delta\sigma_0$	81MPa	278 MPa	For N = 1e9, R = 0, in water max = uncorrected value min = corrected value for P = 95% and Smax = Su	[56]

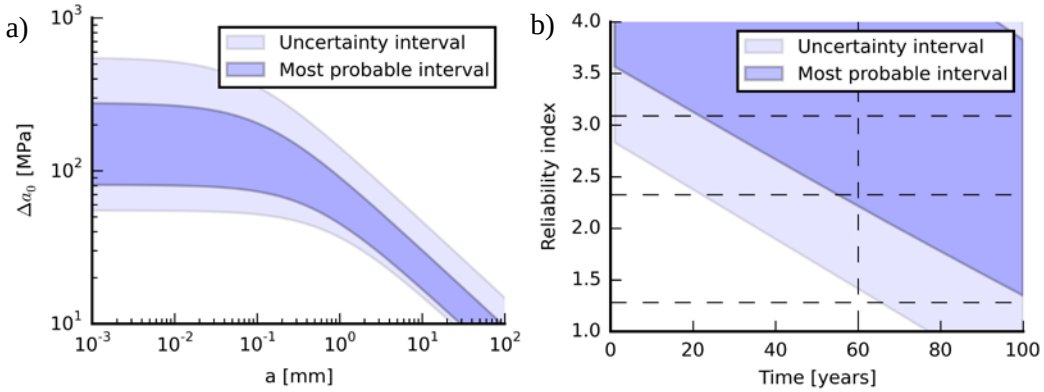

Figure 8. a) Limit state uncertainty interval and most probable interval
b) Evolution of the reliability index over time for both intervals

However, defining smaller probable uncertainty intervals could be hazardous as more information is needed on the materials and the manufacturing processes used during fabrication. Even with this information available, it will be necessary to quantify the effect of the different microstructural features on the limit state and to identify them in the actual steel that is used for a particular runner. This approach also implies that correlations has to be developed between the metrics commonly used to qualify materials during their manufacturing and the microstructural features found to be detrimental to fatigue behaviour.

5. Conclusions

From the sensitivity analysis presented in this paper some conclusions can be drawn about the effect of materials properties on fatigue reliability of turbines:

- Both crack growth threshold and fatigue limit have to be considered to correctly assess the turbine runner reliability in fatigue.
- The crack growth rate has a big influence on the reliability decreasing rate over time.
- For the simplified spectrum used in this study, the most influential property is the crack growth threshold.

This exercise clearly shows how improvements to the materials could be beneficial to fatigue reliability. The brief review of the most influential microstructural features of 13%Cr-4%Ni steels shows that a lot of research work has still to be done on this complex alloy to correctly assess their relative importance. In parallel, finding correlations between metrics commonly used to qualify materials during manufacturing and the microstructural features that will prove to be most influential in regards to fatigue will reduce the limit state uncertainty interval. This will lead to a better evaluation of fatigue reliability of hydraulic turbines and, in the long run, to more durable turbine runners.

Acknowledgments

The authors would like to thank Carlo Baillargeon and Dr. Jacques Lanteigne for the crack growth rate curves and Dr. Pierre Hovington for the help on the scanning microscope.

References

[1] Gagnon M, Tahan A, Bocher P, Thibault D, 2013, A probabilistic model for the onset of High Cycle Fatigue (HCF) crack propagation: Application to hydroelectric turbine runner, *Int. J. Fatigue*, **47**, 300-7

[2] Kitagawa H and Takahashi S, 1976, Applicability of fracture mechanics to very small cracks or the cracks in the early stage, *Second International Conference on Mechanical Behavior of Materials.* , ASM, Metals Park, Ohio, 627-31

[3] Gagnon M, Tahan A, Bocher P and Thibault D, 2013, On the Fatigue Reliability of Hydroelectric Francis Runners, *Procedia Engineering*, **66**, 565-74

[4] Gagnon M, Tahan S, Bocher P and Thibault D, 2012, The role of high cycle fatigue (HCF) onset in Francis runner reliability, *IOP Conference Series: Earth and Environmental Science*, **15**, 022005

[5] Gagnon M, Tahan A, Bocher P and Thibault D, 2014, Influence of load spectrum assumptions on the expected reliability of hydroelectric turbines: A case study, *Structural Safety*, **50**, 1-8

[6] Atzori B and Lazzarin P, 2002, A three-dimensional graphical aid to analyze fatigue crack nucleation and propagation phases under fatigue limit conditions, *Int. J. Fracture*, **118**, 271-84

[7] Thieulot-Laure E, Pommier S and Fréchinet S, 2007, A multiaxial fatigue failure criterion considering the effects of the defects, *Int. J. Fatigue*, **29**, 1996-2004

[8] Sadananda K and Sarkar S, 2013, Modified Kitagawa Diagram and Transition from Crack Nucleation to Crack Propagation, *Metallurgical and Materials Transactions A*, **44**, 1175-89

[9] Sadananda K, Sarkar S, Kujawski D and Vasudevan A, 2009, A two-parameter analysis of fatigue life using $\Delta\sigma$ and σmax, *Int. J. Fatigue*, **31**, 1648-59

[10] Standards B, 2005, *BS7910: 2005 Guide to methods for assessing the acceptability of flaws in metallic structure*,

[11] Lanteigne J, Sabourin M, Bui-Quoc T and Julien D, 2008, The characteristics of the steels used in hydraulic turbine runners, *IAHR 24th Symposium on Hydraulic Machinery and Systems*,

[12] Sabourin M, Thibault D, Bouffard D and Levesque M, 2010, New parameters influencing hydraulic runner lifetime, *IOP Conference Series: Earth and Environmental Science*, **12**, 012050

[13] Sabourin M, Thibault D, Bouffard D-A and Levesque M, 2010, Hydraulic Runner Design Method for Lifetime, *International Journal of Fluid Machinery and Systems*, **3**, 301-8

[14] Thibault D, Bocher P, Thomas M, Lanteigne J, Hovington P and Robichaud P, 2011, Reformed austenite transformation during fatigue crack propagation of 13% Cr–4% Ni stainless steel, *Materials Science and Engineering: A*, **528**, 6519-26

[15] Gysel W, Gerber E and Trautwein A, 1982, CA6NM: New developments based on 20 years' experience, *ASTM STP 756*, 403-35

[16] Nalbone C, 1982, Effects of carbon content and tempering treatment on the mechanical properties and sulfide stress corrosion cracking resistence of AOD-Refined CA6NM, *ASTM*, **756**, 315-31

[17] Folkhard E, 1988, *Welding metallurgy of stainless steels*, Berlin, (Springer-Verlag),

[18] Bilmes P D, Solari M and Llorente C L, 2001, Characteristics and effects of austenite resulting from tempering of 13Cr-NiMo martensitic steel weld metals, *Material Characterization*, **46**, 285-96

[19] Crawford J, 1975, CA6NM -An update, *Steel foundry facts -Steel Founders Society of America*, **313**,

[20] Gooch T G, Woolin P and Haynes A G, 1999, Welding metallurgy of low carbon 13%Cr martensitic steels,

Supermartensitic Stainless Steel, Bruxelles, KCI Publishing BV, 25-32

[21] Kimura M, Miyata Y, Toyooka T and Kitahaba Y, 2001, Effect of retained austenite on corrosion performance for modified 13%Cr steel pipe, *Corrosion*, **57**, 433-9

[22] Marder A and Krauss G, 1967, The morphology of martensite in iron-carbon alloys, *ASM Trans Quart*, **60**, 651-60

[23] Morito S, Tanaka H, Konishi R, Furuhara T and Maki T, 2003, The morphology and crystallography of lath martensite in Fe-C alloys, *Acta Mater.*, **51**, 1789-99

[24] Krauss G, 1999, Martensite in steel: strength and structure, *Materials Science and Engineering A*, **273-275**, 40-57

[25] Morito S, Yoshida H, Maki T and Huang X, 2006, Effect of block size on the strength of lath martensite in low carbon steels, *Materials Science and Engineering: A*, **438**, 237-40

[26] Wang C, Wang M, Shi J, Hui W and Dong H, 2008, Effect of microstructural refinement on the toughness of low carbon martensitic steel, *Scripta Materialia*, **58**, 492-5

[27] Morris Jr J, 2001, The influence of grain size on the mechanical properties of steel,

[28] Nakai Y, Tanaka K and Nakanishi T, 1981, The effects of stress ratio and grain size on near-threshold fatigue crack propagation in low-carbon steel, *Eng. Fract. Mech.*, **15**, 291-302

[29] Masounave J and Bailon J-P, 1976, Effect of grain size on the threshold stress intensity factor in fatigue of a ferritic steel, *Scripta Metall.*, **10**, 165-70

[30] Yoder G, Cooley L and Crooker T, 1983, A Critical Analysis of Grain-Size and Yield-Strength Dependence of Near-Threshold Fatigue Crack Growth in Steels, *Fracture Mechanics: Fourteenth Symposium*, **1**, 348-65

[31] Priddle E, 1978, The influence of grain size on threshold stress intensity for fatigue crack growth in AISI 316 stainless steel, *Scripta Metall.*, **12**, 49-56

[32] Bathias C and Baïlon J P, 1997, *La fatigue des matériaux et des structures*, Paris, (Hermes), **2**,

[33] Ravichandran K, Panchapagesan T and Dwarakadasa E, 1987, The effect of crack closure on the grain size dependence of fatigue crack growth threshold, *Scripta Metall.*, **21**, 919-24

[34] Carlson M and Ritchie R, 1977, On the effect of prior austenite grain size on near-threshold fatigue crack growth, *Scripta Metall.*, **11**, 1113-8

[35] Murakami R and Akizono K, 1981, The influence of prior austenite grain size and stress ratio on near threshold fatigue crack growth behavior in high strength steel, *ICF5, Cannes (France) 1981*,

[36] Tokaji K and Ogawa T, 1992, The growth behaviour of microstructurally small fatigue cracks in metals, *Short fatigue cracks, ESIS*, **13**, 85-99

[37] Trudel A, Lévesque M and Brochu M, 2014, Microstructural effects on the fatigue crack growth resistance of a stainless steel CA6NM weld, *Eng. Fract. Mech.*, **115**, 60-72

[38] Thibault D, Bocher P, Thomas M, Lanteigne J, Hovington P, Robichaud P, 2011, Reformed austenite transformation during fatigue crack propagation of 13%Cr-4%Ni stainless steel, *Materials Science and Engineering: A*, **528**, 6519-26

[39] Song Y, Li X, Rong L, Ping D, Yin F and Li Y, 2010, Formation of the reversed austenite during intercritical tempering in a Fe–13% Cr–4% Ni–Mo martensitic stainless steel, *Materials Letters*, **64**, 1411-4

[40] Bilmes P D, Llorente C L and Pérez-Ipina J, 2000, Toughness and microstructure of 13Cr4NiMo high-strength steel welds, *Journal of Materials Engineering and Performance*, **9**, 609-15

[41] Song Y, Ping D, Yin F, Li X and Li Y, 2010, Microstructural evolution and low temperature impact toughness of a Fe–13% Cr–4% Ni–Mo martensitic stainless steel, *Materials Science and Engineering: A*, **527**, 614-8

[42] Godin S, 2014, *Effet d'un enrichissement en nickel sur la stabilité mécanique de l'austénite de réversion lorsque soumise à de la fatigue oligocyclique*, École de technologie supérieure, Université du Québec, Master's thesis

[43] Robichaud P, 2007, *Caractérisation de la stabilité de l'austénite résiduelle du 415 soumis à un cyclage en fatigue oligocylique*, École de technologie supérieure, Université du Québec, Master's thesis

[44] Chaix J, 2014, *Influence de la température de revenu sur la résistance du CA6NM à la propagation des fissures de fatigue*, École Polytechnique de Montréal, M.Sc.

[45] Wang P, Lu S, Xiao N, Li D and Li Y, 2010, Effect of delta ferrite on impact properties of low carbon 13Cr–4Ni martensitic stainless steel, *Materials Science and Engineering: A*, **527**, 3210-6

[46] Carrouge D, Bhadeshia K D H and Woollin P, 2004, Effect of δ-ferrite on impact properties of supermartensitic stainless steel heat affected zones, *Science and Technology of Welding and Joining*, **9**, 377-89

[47] Wilson A, 1981, Fractographic characterization of the effect of inclusions on fatigue crack propagation, *Fractography and Materials Science, ASTM STP*, **733**, 166-86

[48] Fowler G J, 1979, The influence of non-metallic inclusions on the threshold behavior in fatigue, *Materials Science and Engineering*, **39**, 121-6

[49] Atkinson H and Shi G, 2003, Characterization of inclusions in clean steels: a review including the statistics of extremes methods, *Progress in Materials Science*, **48**, 457-520

[50] Murakami Y, 2002, *Metal fatigue: effects of small defects and nonmetallic inclusions: effects of small defects and nonmetallic inclusions*, (Elsevier),

[51] Murakami Y, Toriyama T, Tsubota K, Furumura K and Tanaka K, 1998, What Happens to the Fatigue Limit of Bearing Steel Without Nonmetallic Inclusions?: Fatigue Strength of Electron Beam Remelted Super Clean Bearing Steel, *ASTM SPECIAL TECHNICAL PUBLICATION*, **1327**, 87-108

[52] 2007, *ASME Boiler and Pressure Vessel Code Section VIII, Division 2*,

[53] Aven T, Zio E, Baraldi P and Flage R, 2013, *Uncertainty in risk assessment : The representation and treatment of uncertainties by probablilistic and non-probabilistic methods*, (John Wiley & Sons),

[54] Tanaka K, Yamaguchi N, Fujiki S, Furoya S, Tsunoda S and Yamagata I, 1992, Studies on dynamic stress of runners for

the design of 760 metre head pump-turbine, Sao Paulo,

[55] Usami S and Shida S, 1982, Effects of environment, stress ratio and defect size on fatigue threshold, *Journal of Japan Society of Materials*, **31**,

[56] Mahnig F, Rist A and Walter H, 1974, Strength and mechanical fracture behaviour of cast steel for turbines -Part One, *Water Power 1074*, 338-42